Phaseic acid: an endogenous and reversible inhibitor of glutamate receptors in mouse brain

Hou, Sheng T.; Jiang, Susan X.; Zaharia, L. Irina; Han, Xiumei; Benson, Chantel L.; Slinn, Jacqueline; Abrams, Suzanne R.

Publisher's version / Version de l'éditeur:
https://doi.org/10.1074/jbc.M116.756429
The Journal of Biological Chemistry, 291, 53, pp. 27007-27002, 2016-11-18

JBC Papers in Press. Published on November 18, 2016 as Manuscript M116.756429
The latest version is at http://www.jbc.org/cgi/doi/10.1074/jbc.M116.756429

Phaseic Acid: An Endogenous and Reversible Inhibitor of Glutamate Receptors in Mouse Brain

Sheng T. Hou[1,2,4†], Susan X. Jiang[2], L. Irina Zaharia[3], Xiumei Han[3], Chantel L. Benson[3], Jacqueline Slinn[2], Suzanne R. Abrams[3,‡],

From [1] Brain Research Centre and Department of Biology, Southern University of Science and Technology, 1088 Xueyuan Blvd, Nanshan District, Shenzhen, Guangdong Province, P. R. China, 518055
[2]Experimental NeuroTherapeutics, Human Health Therapeutics Portfolio, National Research Council Canada, 1200 Montreal Road, Bldg M54, Ottawa, Ontario, Canada, K1A 0R6;
[3] Aquatic and Crop Resource Development, National Research Council Canada; 110 Gymnasium Place, Saskatoon, Saskatchewan, Canada, S7N 0W9;
[4]Department of Biochemistry, Microbiology and Immunology, Faculty of Medicine, University of Ottawa, Ontario, Canada; K1H 8M5

Running title: *Phaseic acid in mouse brain*

†To whom correspondence should be addressed: Prof. Sheng T. Hou, Ph. D.; Brain Research Centre and Department of Biology, Southern University of Science and Technology, 1088 Xueyuan Blvd, Nanshan District, Shenzhen, Guangdong Province, P. R. China, 518055
Tel: 86-755-8801-8418; Email: hou.st@sustc.edu.cn

Keywords: Phaseic acid; abscisic acid; UPLC/MS/MS; endothelial cells; choroid plexus; cerebrospinal fluid; cerebral ischemia.

ABSTRACT

Phaseic acid (PA) is a phytohormone regulating important physiological functions in higher plants. Here, we show the presence of naturally occurring (-)-PA in mouse and rat brains. (-)-PA is exclusively present in the choroid plexus and the cerebral vascular endothelial cells. Purified (-)-PA has no toxicity and protects cultured cortical neurons against glutamate toxicity through reversible inhibition of glutamate receptors. Focal occlusion of the middle cerebral artery (MCAO) elicited a significant induction in (-)-PA expression in the CSF, but not in the peripheral blood. Importantly, (-)-PA induction only occurred in the penumbra area, indicting a protective role of PA in the brain. Indeed, elevating (-)-PA level in the brain reduced ischemic brain injury, while reducing (-)-PA level using a monoclonal antibody against (-)-PA increased ischemic injury. Collectively, these studies showed for the first time that (-)-PA is an endogenous neuroprotective molecule capable of reversible inhibiting glutamate receptors during ischemic brain injury.

INTRODUCTION

Phaseic acid (PA), a terpenoid catabolite of abscisic acid (ABA), is generated spontaneously after 8'-hydroxylation of ABA by cytochrome P450s in the CYP707A subfamily (1). In higher plants, PA and ABA act as phytohormones regulating important physiological functions in growth and development, as well as in responses to biotic and abiotic stress (cold, drought, heat exposure, salinity). The regulation of these processes is mediated by a change in endogenous PA and ABA levels that are controlled by the balance between biosynthesis and metabolism. ABA induces the production of the second-messenger, cyclic ADP ribose, which controls the release of stored intracellular calcium in plants to exert its effect (2-4).

ABA in plants can be metabolized by conjugation and oxidation. The principal oxidative pathway of natural (+)-ABA, mediated by cytochrome P-450 monooxygenases, occurs through hydroxylation of the 8'-methyl group resulting in 8'-hydroxyABA, which rearranges to (-)-PA (1). Further enzymatic reduction of (-)-PA leads to the production of DPA. Similar to ABA, naturally occurring (-)-PA is a plant hormone associated with photosynthesis arrest and abscission (5). However, very little is known about the presence and function of PA in the mammalian system.

Stroke is a leading cause of death and disability in the world. However, protecting stroke-induced brain injury still represents one of the largest unmet medical needs (6,7). Despite of decades of effort trying to find ways to protect neurons against ischemic insult, no clinical effective drugs are available. It is known that brain can indeed launch an internal protective response against ischemic insult, such as activating autophagy machinery (8). However, in general, the brain's endogenous protective mechanisms against cerebral ischemia remain not well understood. Further understating the internal defense system would be extremely beneficial to develop appropriate drugs against stroke in humans.

Cerebral ischemia induces rapid neuronal cell membrane depolarization and activates NMDA-type glutamate receptors (NMDARs). Subsequent increased calcium influx through NMDARs causes excitotoxicity, a process which is toxic to neurons and contributes to a wide range of neurological disorders such as cerebral ischemia (6,9,10). Although drugs directly blocking NMDARs are effective in neuroprotection, all have failed to be approved for clinical use due to their severe side effects affecting normal physiological functions of NMDARs. It has been suggested that compounds with properties to reversible and uncompetitive blocking NMDAR are the preferred candidates for development as therapeutics against stroke (9).

Because ABA and PA are known to modulate the release of intracellularly stored calcium to affect plant guard cell death and

leaf dropping, we hypothesised that ABA and its metabolites might be involved in animal cells calcium regulation. In particular, the presence of ABA has been shown in the brains of pigs and rats (11), it is therefore highly possible that the surge in intracellular calcium following cerebral ischemia in the ischemic core in the brain can be affected by the presence of ABA and its metabolites. Indeed, our data showed the presence of surprisingly high level of endogenous (-)-PA, but not other ABAs, in the choroid plexus, CSF and vascular endothelial cells in ischemic mouse and rat brains. The localization of (-)-PA is only in the penumbra area surrounding the ischemic infarct core, indicating its involvement in neuroprotection. Interestingly, (-)-PA reversibly inhibits glutamate receptors, reduces intracellular calcium influx and protects cortical neurons against glutamate toxicity *in vitro* and *in vivo*. These studies revealed a previously unknown role of PA serving as an endogenous mechanism of neuroprotection in ischemic brain, and suggest that (-)-PA or its analogous can be developed as a powerful agent for neuroprotection against stroke.

RESULTS

The presence of (-)-PA in mouse and rat brains - We have successfully developed methods to analyze and quantify PA and its metabolites in mouse and rat brain tissues, using ultra performance liquid chromatography coupled with tandem mass spectrometry (UPLC/MS/MS). Deuterium-labeled internal standards were used and spiked in samples to confirm the identity of PA species (Fig 1). Levels of PA, DPA, ABA, 7'OH-ABA, *neo*PA, ABAGE and *trans*-ABA from both mouse brain and blood were accurately measured and quantified against dry sample weight (DW) using UPLC/MS/MS (Fig 2).

To determine the stereochemical nature of the observed PA, tissue samples were chromatographed using a chiral column and the identity of the observed PA was checked against synthetic standards of the natural form of PA: (-)-PA, and the unnatural mirror-image form of PA: (+)-PA (Fig 1A and B). Near baseline enantioseparation of PA in standard solutions was achieved by a gradient elution mode as described in the Material and Methods section. The chromatograms of PA in mouse brain tissue and blood samples were compared to that of the known standards. Spiking experiments of brain and blood samples with known amounts of natural (-)-PA standard resulted in the corresponding increase of the PA signal in the mouse brain tissue and mouse blood confirming the same stereochemistry as the plant-derived compound. The chromatograms of (-)-PA in rat brain tissue, CSF, and blood samples were also compared to that of the known standards. Spiking experiments of rat CSF, blood and samples with known amounts of natural (-)-PA standard also resulted in the corresponding increase of the PA signal in the rat CSF, blood and brain confirming the same stereochemistry as the plant-derived compound (Fig 1D). Based on the spiking experiment using the two forms of PA standards shown in Fig 1B-D, it is clear that mouse and rat only produce (-)-PA, the naturally occurring form of PA in the brain, CSF and blood.

Mouse brain contains a small amount of ABA (74.9 ± 45.2 ng/g DW; n = 12), which was in agreement with an earlier report on the presence of ABA in pig and rat brains (11). However, brain ABA level was close to 30 times lower compared with that of (-)-PA (2245.20 ± 573.20 ng/g DW; n = 15) (Fig 2A). High level of (-)-PA was consistently detected in both the right and left hemispheres of the brain. Mouse blood does contain (-)-PA, but the level of which was 10 fold lower compared to that found in the brain tissue (232.20 ± 90.68 ng/g DW; n = 4; as shown in Fig 2A, $p > 0.01$, paired t-test). All other ABA metabolites were also present in extremely low quantities in the blood of mouse fed with standard diet.

(-)-PA is endogenously produced in the brain-To determine the source of mouse brain (-)-PA, we tested the content of ABA

derivatives in mouse food pellet. Mouse food was obtained from a commercial source with fixed ingredients. As shown in Fig 2B, standard mouse food pellet contains very low level of ABA and PA. Analysis of the food pellets showed the presence of low amounts of DPA (341 ng/g DW), PA (27 ng/g DW), ABA (42 ng/g DW), neo-PA (36 ng/g DW) and trans-ABA (47 ng/g DW) (Fig 2B). This result argues against the assumption that brain (-)-PA might be the result of accumulation of ABA from food sources.

Moreover, to determine if food born ABA can even be converted to (-)-PA and be accumulated in the brain, mice were injected through i.v with purified (+)-ABA and (-)-ABA at 45 mg/kg or 112.5 mg/kg each (Fig 2C). These high amounts of ABA were arbitrarily used into order to detect a surge of their derivatives in the brain. Ethanol (2%), or saline, used as solvents for ABA, was also injected in mice serving as controls. No clear increase in PA or DPA occurred in mouse brain tissues. Only induction of (+)-ABA and ABAGE was observed in mouse brain after 2 h injection of ABA and both decreased significantly after 5 h of injection in the brain, indicating that the high level of (-)-PA occurring in mouse brain was in fact produced endogenously in the brain. Together these data supports the fact that brain (-)-PA could not have derived from external sources.

The presence of (-)-PA in CSF, choroid plexus and cerebral vascular endothelial cells-To demonstrate where (-)-PA is exactly localized in the brain, a mouse monoclonal antibody made specific to PA was used (12). This antibody cross-reacts with both forms of PA, but does not react with ABA, nor with DPA (12). Because our UPLC/MS/MS detected the presence of only (-)-PA in muse and rat brain tissues and the blood, it is assumed that PA antibody reactivity would represent that from (-)-PA. The specificity of the PA antibody to mouse brain tissue was confirmed using an immunosorbent assay to remove the primary or secondary antibody to yield negative staining on an indirect immunofluorescent assay (not shown). Strong PA immunofluorescence was detected in the brain ventricles associated with the choroid plexus (Fig 3A-C) and on the cerebral vascular walls (Fig 3D-J). Double immonostaining with antibodies specific to choroid plexus cells (TTR) and PA confirmed confirmed co-localization of PA with choroid plexus epithelial cells (Fig 3B, B'). Higher magnification of the choroid plexus immunostaining showed that PA appeared in the cytoplasm of all cells lining the choroid plexus. Furthermore, PA double-immunostaining staining positively co-localizes PA with those of CD31 and Lectin (Fig 3D-I), but not PDGFRβ, GFAP, NeuN, and IBA-1 (Fig 3J-M), indicating that PA was endogenously produced in the brain by choroid plexus and vascular endothelial cells.

Cerebral ischemia induces (-)-PA production in the CSF and ischemic penumbra -In order to determine the function of (-)-PA in the brain, mouse and rat MCAO models were used in the study (Fig 4A). MCAO elicited significant increase in the level of (-)-PA after 2 h reperfusion in the ischemic mouse brain (Fig 4B). The (-)-PA level reached peak at 24 h reperfusion and gradually decreased in both cortices to basal level after 28 d reperfusion (Fig 4B).

The presence of (-)-PA in rat ischemic brain (Fig 4C), and in rat CSF (Fig 4D), but not in rat peripheral blood (Fig 4D), also increased significantly after 24 h reperfusion. Because of technical difficulties obtaining adequate quantities of CSF from the mouse brain, only rat CSF was collected and quantified using UPLC/MS/MS. As shown in Fig 4D, rat CSF contains comparable level of (-)-PA found in the brain, but significantly higher level of (-)-PA compared to that in the blood (Fig 4D). Together, it is very interesting that MCAO treatment induced (-)-PA expression in both the contralateral and ischemic side of the brain, indicating that (-)-PA might play a protective role in the ischemic brain.

To establish the exact location of (-)-PA in the ischemic mouse brain, double-immunohistochemical staining for PA was performed (Fig 5). PA immunofluorescence

increased dramatically in the penumbra area (area 3 in Fig 5A, F) compared with the ischemia infarct core (area 2 in Fig 5A and E) and the sham-operated mouse brain (Fig 5C and J). Using tissue laser capture microdissection techniques, we collected brain tissues from the ischemic core (Fig 5A area 2), the penumbra (Fig 5A area 3), the contralateral side (Fig 5A area 4), and the sham brain for UPLC/MS/MS analysis. The result showed that (-)-PA level was significantly higher in the penumbra and contralateral side of the brain than that in the ischemic core (Fig 5J). Cerebral vascular localization of PA was also much pronounced in the penumbra area (Fig 5G-I) based on double-immunostaining. These studies indicated that the naturally occurring (-)-PA may play an importantrole in the ischemic brain.

(-)-PA reversibly inhibits glutamate receptors-Glutamate-mediated excitotoxicity plays a major role in ischemic neuronal injury (6,7). Compounds reversible inhibiting glutamate receptors protects brain from ischemic damage (9,10). Experiments were therefore designed to determine if (-)-PA has any effect on cortical glutamate receptors. Based on results derived from the following two experiments, it is clear that (-)-PA functions as a reversible glutamate receptor inhibitor.

First, ratiometric calcium assay using Fura2-AM showed that (-)-PA dose-dependently decreased cortical neuronal intracellular calcium ($[Ca^{2+}]i$) influx when treated with 100 μM NMDA (Fig 6A, B). (-)-PA alone ranging from 10 μM to 1000 μM didn't affect neuronal $[Ca^{2+}]i$, but effectively reduced NMDA-induced increase in $[Ca^{2+}]i$. Interestingly, inhibition of $[Ca^{2+}]i$ by (-)-PA was reversible and (-)-PA's effect can be washed off using culture media. Subsequently, neurons showed a strong surge of $[Ca^{2+}]i$ in response to KCl depolarization, serving as a control (Fig 6A). The fold of reduction of $[Ca^{2+}]i$ by (-)-PA was quantified from measurements of at least 20 cells and shown in Fig 6B. These observations suggested that (-)-PA is a potential reversible inhibitor of glutamate receptors.

Second, whole-cell patch-clamp recordings demonstrated a dose-dependent inhibition of NMDA-activated currents by (-)-PA (Fig 6C, D, E). The effect of (-)-PA and NMDA on neuronal excitability was first determined in cultured cortical neurons. As shown in Fig. 6C, 50 μM NMDA plus 1 μM glycine induced a large inward current at −50 mV. In contrast, application of (-)-PA with a series of concentrations in the range between 10 –1000 μM neither induced any detectable current at −50 mV, nor affected the membrane potential (not shown). To determine the effect of (-)-PA on NMDA-activated current, the dose-response relationship was established by application of NMDA for 30 s followed by addition of (-)-PA (Fig. 6C, D). (-)-PA inhibited NMDA-activated current in a dose-dependent manner (Fig. 6E) over the range of 100–1000 μM with an IC_{50} of 35.4 ± 1.5 μM and a slope factor of 0.96 ± 0.3 (n=10). This inhibition was fully reversible after a few seconds of washing. Results from these experiments showed that (-)-PA not only dose-dependently, but also in a reversible manner, inhibited NMDA current. When (-)-PA and NMDA were removed, the membrane potential returned fully to the normal resting level.

Together these experiments demonstrated that (-)-PA reversible and transiently blocks glutamate receptors and potentially plays a key role in preventing excitotoxicity in the ischemic brain.

(-)-PA protects cortical neurons against glutamate toxicity--Cultured cortical neurons undergo cell death in response to bath incubation with NMDA at 100 μM for 6 h (Fig 7A). Pre-treatment of neurons with (-)-PA inhibitedneuronal death dose-dependently against NMDA toxicity (Fig 7B). Both phase contrast and DAPI staining images were shown in Fig 7 C. (-)-PA itself has no toxicity to cultured neurons (Fig 7A). A calpain inhibitor, ALLN, was very effective in neuroprotection against NMDA toxicity to neurons (Fig 7B), serving as a positive control.

Elevation of (-)-PA level reduced ischemic brain injury--To determine if (-)-PA was indeed protective against cerebral ischemia, (-)-PA was delivered to the mouse brain using a pre-implanted osmotic pump through a cannula to the left cerebral ventricle on the ischemic side of the brain. Mice treated with (-)-PA and vehicle had a similar survival rate, as this particular MCAO mouse model has very small death rate over the period of surgery and recovery (Fig 7D). Mice receiving (-)-PA showed no change in survival rate compared to the vehicle-treated group of mice serving as a control. However, the ischemic infarct size was significantly reduced in (-)-PA-treated group after 24 d reperfusion (Fig 7E). Furthermore, (-)-PA-treated mice showed significantly better improvement in neurological scores (Fig 7F). These results indicated that (-)-PA is neuroprotective.

Reduction in (-)-PA level in the brain worsens MCAO outcomes-Monoclonal antibody against PA was delivered to the brain left ventricle right before MCAO using a pre-implanted osmotic pump through a cannula to the left cerebral ventricle on the ischemic side of the brain. After 24 d reperfusion, TTC staining of the ischemic brain showed a much enlarged ischemic infarct core compared with the vehicle-treated group (Fig 8A and B). Indeed, PA antibody-treated group exhibited significant deterioration of neurological deficit scores (Fig 8C) and reduced forepaw pulling strength (Fig 8D) following MCAO, indicating that reduced PA expression in the brain worsens neurological outcomes of cerebral ischemia. Mice receiving PA Ab, but not MCAO, had no effect on the survival rate, neurological scores, nor brain tissue damage, serving as a control.

To confirm the level of (-)-PA in the brain after antibody treatment, immunostaining was performed to demonstrate the reduction of PA expression levels in both of the ischemic infarct core tissue (Fig 8E, F) and the penumbral tissue (Fig 8E, G). To compare with a control group without PA antibody treatment, please see Fig 5D,E,F. Tissue microdissection was used to isolate brain tissue from these areas and subjected them to UPLC/MS/MS analysis (Fig 8H). Indeed, infusion of PA antibody to the brain inhibited the rise of (-)-PA level in the ischemic mouse brain.

DISCUSSION

In the present study, we profiled the presence of plant stress hormone, PA and all major ABA metabolites, in mouse and rat brains. Except for (-)-PA, no other plant ABA metabolites appear to be present in quantifiable amounts in rat and mouse brain and blood. (-)-PA occurs in high quantities in rodent brain tissues relative to a much lower level of (-)-PA in the peripheral blood. Cerebral ischemia evoked a significant increase in (-)-PA in the ischemic brain penumbra, particularly in the CSF, compared to the sham-operated animals. Brain (-)-PA was from endogenous sources (cerebral endothelial cells and the choroid plexus), rather than exogenous sources (such as accumulation from food). Importantly, endogenously produced (-)-PA plays a role in reversibly blocking glutamate receptors during cerebral ischemia in tissues surrounding the ischemic core, suggesting that naturally occurring (-)-PA is an endogenous neuroprotectant to the brain. To the best of our knowledge, this is the first report of the presence of (-)-PA in rodent brains. It is especially intriguing as to the presence of high level of (-)-PA in the CSF of ischemic brains, which may represent an internal defence system during brain injury. The utility of these findings warrants further investigation.

Is (-)-PA in the brain derived from ABA metabolism? ABA in plants can be metabolized by conjugation and oxidation. The principal oxidative pathway of natural (+)-ABA is mediated by cytochrome P-450 monooxygenases (Fig 9, **1**) (Krochko et al., 1998) through hydroxylation of the 8'-methyl group. The resulting 8'-hydroxyABA can be rearranged to PA. Further enzymatic reduction of PA leads to DPA (Fig 9, **4**). Other metabolic steps, as reviewed in (13,14), include hydroxylation of the 7' and

9'-methyl groups of the ABA ring as well as conjugation as glucose esters (ABAGE). *Trans*-ABA is a product of isomerization of natural ABA under UV light. In plants, the unnatural mirror-image form (-)-ABA is mainly metabolized by hydroxylation at the 7'-methyl group, but there are also reports of the unnatural mirror-image form of PA (Fig 9, **7**) as a minor product which resulted from the feeding of unnatural (-)-ABA to maize cell suspension culture (15).

Although it is not possible to fully discard an external source of (-)-PA as we still do not have any direct proof of local production, based on the current study, it is highly unlikely that the high level of naturally occurring (-)-PA was the result of ABA metabolism in the brain. First, both mouse and rat brains and their blood contain very low levels of ABA and its intermediates. Even injection of large quantities of (+)-ABA and (-)-ABA into the blood stream failed to produce noticeable increase in (-)-PA level. Second, (-)-PA level in the brain was at close to 2500 times higher than that of ABA, while ABA level in mouse and rat tissues were almost undetectable. This makes it inconceivable for such a low amount of ABA to be transformed into the high level of (-)-PA. Third, mouse food has extremely low level of ABA and almost undetectable amount of (-)-PA, confirming a previous report by Le Page-Degivry et al (11) which showed that the low level of ABA contents of the rat brain tissue were not correlated with the amount of ABA in the diet, as animals fed for two generations on a synthetic ABA-poor diet had more ABA in their brains than control animals. We show here that, apart from very low levels of DPA and traces of ABA and *trans*-ABA, no other ABA metabolites were present in quantifiable amounts in the mouse food. Fourth, our results showed that in the ischemic brain, (-)-PA levels significantly increased. Interestingly, the induction in (-)-PA in the ischemic brain was not followed by the increase in any other ABA metabolites, not even DPA, the downstream product of PA in the ABA metabolism pathway known in plants. This suggests that (-)-PA was either transported from elsewhere, such as the CSF or is possibly following an alternate metabolic pathway different from that in plants. Therefore, the only plausible conclusion from these studies is that the high levels of (-)-PA seen in rodent brains could only be generated from endogenous sources. Indeed, double immunostaining and confocal fluorescence microscopy data lend further support to the argument that (-)-PA in the CSF was derived from the choroid plexus and brain endothelial cells.

What are the patho-physiological functions of brain (-)-PA? Cerebral ischemia initiates a complex cascade of biochemical events, amongst which the excessive release of glutamate and its induction of excitotoxicity represent a major and early response in the brain (6). Over-stimulation of NMDA receptors with glutamate results in an excessive influx of $[Ca^{2+}]i$. Increased $[Ca^{2+}]i$ activates a plethora of potentially neurotoxic mechanisms, such as the early induction of a calcium-dependent protease, calpain, which cleaves intracellular structural proteins such as spectrin, causing the collapse of intracellular structures and eventually neuronal death. Excitotoxicity contributes to a wide range of neurological disorders, such as stroke. Pharmacological inhibition of NMDAR ameliorates excitotoxicity-mediated neuronal death and protects the brain after cerebral ischemia (7). Given that calcium imaging and whole cell recording techniques showed that (-)-PA dose-dependently blocks NMDA receptors, it is determined that (-)-PA plays a key role in modulating NMDA receptors. The fact that (-)-PA is present in great quantities in both the viable brain tissues surrounding the ischemic core and in the contralateral side of the brain strongly suggest that (-)-PA may play a role in protecting neurons. Indeed, injection of purified (-)-PA protected mouse brain against MCAO, while administering of an antibody against (-)-PA exacerbated brain injury following MCAO. It is also intriguing as to why (-)-PA was also present in the contralateral side of the brain. Based on immunostaining and MS analysis, a major site (-)-PA production was traced to choroid plexus. Rat CSF contains a very high level of

(-)-PA. During ischemic reperfusion, increased (-)-PA may be circulated with CSF into both the ipsilateral and contralateral side of the brain.

What is the potential implications of (-)-PA as an endogenous inhibitor against NMDA receptors? Agents that inhibit NMDA receptors in a transient and reversible manner are of significant interests for drug development against glutamate toxicity (9,10). Because these drugs uncompetitively inhibit NMDA receptor functions and do not interfere with NMDA receptor physiological functions. Our studies showed that (-)-PA has similar electrophysiological profiles in NMDA receptor inhibition to that of memantine, a gold standard in uncompetitive NMDAR inhibition. Although whether PA acts uncompetitively at NMDA receptors needs to be demonstrated, it is highly possible that induction of (-)-PA by choroid plexus in response to cerebral ischemia represents an endogenous stress response in the brain. Increased level of (-)-PA outside of the ischemic core and the contralateral side of the brain tissue provides an endogenous defence mechanism for brain protection. These findings are novel and potentially important in developing (-)-PA and its analogous as neuroprotectants in treatment of stroke.

EXPERIMENTAL PROCEDURES

Materials-ABA metabolites standards DPA, ABA-GE, PA, 7'- OH-ABA, neoPA, and trans-ABA were synthesized and prepared at the National Research Council of Canada, Saskatoon, Canada, while (±)-ABA was purchased from Sigma–Aldrich. Deuterated forms of the hormones used as internal standards included: d3-DPA, d5-ABA-GE, d3-PA, d4-7'-OH-ABA, d3-neoPA, d4-ABA, and d4-trans-ABA. These hormones were synthesized and prepared as previously published (16). The deuterated forms of the selected hormones used as recovery (external) standards were: d6-ABA and d2-ABA-GE, also prepared and synthesized at the National Research Council of Canada, Saskatoon. Antibodies and their conditions of usage were described in Table 1.

Animal study design-The clinical failure of many candidate drugs that showed promise in acute experimental cerebral ischemia underscores the importance of rigorous and comprehensive preclinical testing along published guidelines and recommendations by expert panels, including STAIR (17,18) and ARRIVE (19). Therefore, we randomized and concealed allocation to treatment groups, reported all mortality as well as attrition due to other causes, and analyzed the data according to intention-to-treat principle and did not exclude animals showing signs of adverse effects such as vomiting or aspiration. Multiple experimenters blinded to the treatment group performed surgeries, assessed endpoints and administered all compounds as (-)-PA and other ABAs in solution can't be distinguished from the vehicle by their colors.

Animal surgery and mouse middle cerebral artery occlusion (MCAO)-All procedures using animals were approved by the HHT Animal Care Committee following the guidelines established by the Canadian Council on Animal Care. C57B/6 mice (20 - 23 g) were obtained from Charles River and bred locally. Under temporary isofluorane anesthesia, MCAO was induced by the intraluminal insertion of a silicon-coated nylon filament (Re L910 PK5, Doccol Corporation) through the common carotid artery into the internal carotid artery and left in place for 60 min as we previously described (20-26). Cerebral blood flow (CBF) was monitored by laser Doppler flowmetry using a probe located in the ipsilateral parietal bone (1–2 mm posterior to bregma), and a >90% reduction in CSF was considered to indicate successful occlusion. The head temperatures were maintained at 37 °C using a warming lamp. Sham animals were generated by the insertion of a filament into the internal carotid artery which was immediately withdrawn.

After 1 h of MCAO, the filament was withdrawn, blood flow was restored to normal, monitored by laser Doppler flowmetry, and wounds were sutured. The body temperature of the experimental animal was monitored before and after the MCAO surgery using a

rectal probe and was maintained at 37 °C using a heating pad and lamp. In preliminary experiments to verify a consistent stroke procedure, measurements of blood pressure, blood gases, and pH were also performed as previously described (27-29). Blood was collected from the facial vein and kept at -80 °C. Brains were removed after 2 h, 6 h, 24 h, 3 d, 7 d and 28 d reperfusion and the right and left hemispheres were isolated. Brain and blood samples were rapidly frozen in liquid nitrogen and stored at -80 °C until they were lyophilized.

Rat focal MCAO-Male Sprague Dawley rats (Charles River) between 350-375 g were kept on a 12 h light-dark cycle and group-housed in plastic cages. Rats were allowed free access to food and water. A total of 20 rats were used and randomly separated into sham and ischemia groups. Each rat was anesthetized with isoflurane followed by a MCAO using procedures modified from previously described (28,29). A 1 cm incision was made midway between the left eye and the external auditory canal to expose the skull. The left middle cerebral artery (MCA) was exposed through a 2 mm burr hole in the skull 2 - 3 mm rastral to the fusion of the zygomatic arch with the squamosal bone. A 1 mm Codman micro-aneurysm clip was applied to the vessel and the wound was closed with suture material. A 1.5 cm incision was made in the ventral surface of the neck. The right and left common carotid arteries were isolated and ligated for two hours using atraumatic clips. During the surgical procedure the rat's body temperature was maintained between 37 - 37.5 °C. At the end of two hours, the carotid clips were removed, the neck wound closed and the animal was returned to its cage and allowed to recover for 24 h. This procedure reduced regional cerebral blood flow to 15% of basal level during the ischemic period and returned it to 95% of basal level upon reperfusion. Body temperature was controlled to 37.5 ± 0.5°C both during anesthesia and after recovery. At 24 h MCAO/reperfusion, the 1 mm Codman micro-aneurysm clip at the left middle cerebral artery was carefully removed and the CSF and brain tissue were collected after euthanization of the rat. The brain was removed and sliced in a rat brain matrix. Brain slices were stained with TTC to confirm the ischemic injury (infarct) with edema subtracted. The rest of the brain tissue was transferred into Eppendorf tubes and frozen at -80 °C.

Infarct size measurement-Infarct size was measured by a colorimetric staining method using 2,3,5-triphenyltetrazolium chloride (TTC) as described previously (25). Briefly, brains were dissected out and cut into four 2-mm-thick coronal slices, which were stained with 5 ml of 2% TTC for 90 min at 37 °C. Afterward, the tissue was rinsed with saline and subsequently exposed to a mixture of ethanol/dimethyl sulfoxide (1:1), which was to solubilize the formazan product. After 24-h incubation in the dark, the red solvent extracts were diluted 1:20 with fresh ethanol/Me_2SO solvent in three tubes and placed in cuvettes. Absorbance was measured at 485 nm in a spectrophotometer and the values were averaged. Percentage loss in brain TTC staining in the ischemic side of the brain was compared with the contralateral side of the brain of the same animal using the following equation: % loss = (1 – (absorbance of ischemic hemisphere/absorbance of contralateral hemisphere) × 100).

Neurological deficit scores-Both a six-point scale assessment and forelimb grip strength test were performed. (a) An expanded six-point scale turning behavior test was used exactly as described previously (21,30). Briefly, behavioral assessments were carried out 30 min after MCAO when animals were fully awake after anesthesia. Assessments were made by an individual blinded to the treatment of the mice. The neurological deficits were scored as follows: 0, normal; 1, mild turning behavior with or without inconsistent curling when picked up by tail, 50% attempts to curl to the contralateral side; 2, mild consistent curling, 50% attempts to curl to contralateral side; 3, strong and immediate consistent curling, mouse holds curled position for more than 1–2 s, the nose of the mouse almost reaches the tail; 4, severe curling progressing into barreling, loss of walking or righting reflex; 5, comatose or moribund. At least eight mice per group were

evaluated and scores were averaged for statistical analysis. (b) Forelimb grip strength test was performed using the Grip Strength Meter from Columbus Instruments (MyNeurolab, St. Louis, MO) which measures muscle strength and neuromuscular integration relating to the grasping reflex in the forepaws. The peak preamplifier automatically stores the peak pull force and shows it on a liquid crystal display. For each animal, at least 10 measurements were taken at a specific time point and the mean and standard error were calculated.

Rat CSF collection-Each rat was anesthetized with isoflurane and the head was flexed downward at approximately 45 degrees on a homemade device. A small midline incision was made beginning between the ears. A retractor was placed with the spring side pointing in the rostral direction. The separation of the superficial muscles exposed an underlying layer of muscles which was easily separated along the midline by blunt dissection. The atlanto-occipital membrane in between the occipital bone and the upper cervical vertebra was exposed. A butterfly needle (25 G x 19 mm) connected to a 1 ml syringe was used. The needle was directly punctured into the cisterna magna, and the clear CSF sample (100 - 250 µl) was drawn into the syringe until blood appeared 37. A hemostat was used to clamp the silicon tubing as soon as blood appeared in CSF. The tube was then cut using scissors from the clear part to avoid blood contamination. The clear CSF was transferred into an Eppendorf tube and the sample was kept frozen at −80 °C for further analysis. Blood samples were collected by heart puncture. The rat was killed by decapitation under anesthesia.

Extraction of PA and ABA metabolites from the brain, blood, CSF and mouse food samples-Freeze-dried tissue was homogenized using a multi-tube ball mill (Mini-BeadBeater-96, Biospec Products Inc., Bartlesville, Oklahoma, USA) and about 50 mg (or less, in the case of CSF) per sample was weighed out into individual Falcon tubes. An aliquot (100 µL) containing all internal standards (d3-DPA, d5-ABAGE, d3-PA, d4-7'OH-ABA, d3-neoPA, d4-ABA and d4-trans-ABA, each at a concentration of 0.2 ng/µL, dissolved in water:acetonitrile,1:1, v/v, with 0.5% glacial acetic acid), was added to each sample, followed by the extraction solvent (3 mL isopropanol : water : glacial acetic acid, 80 :19 : 1, v/v). For the blood and CSF samples the aqueous component (600 µL acidified water) of the extraction solvent was initially added, followed by the combined internal standard aliquot and the organic solvent portion of the extraction solvent (2.4 mL isopropanol with 0.5% glacial acetic acid). After shaking in the dark for 24 h at 4 ºC, samples were centrifuged and the supernatant was isolated and dried on a Büchi Syncore Polyvap (Büchi, Switzerland). Samples were reconstituted in 100 µL methanol/glacial acetic acid (99:1, v/v) followed by 900 µL of aqueous 1% glacial acetic acid, and then partitioned twice against 2 mL hexane. After separation, the aqueous layer was isolated and dried as described above. Dry samples were re-dissolved in 100 µL methanol/glacial acetic acid (99:1, v/v) followed by 900 µL of aqueous 1% glacial acetic acid. The reconstituted samples were passed through equilibrated Oasis HLB cartridges (Waters, Mississauga, ON, Canada), with the eluate acetonitrile:water:glacial acetic acid at 30:69:1 (v/v/v) being dried on a LABCONCO centrivap concentrator (Labconco Corporation, Kansas City, MO, USA). An internal standard blank was prepared with 100 µL of the deuterated internal standards mixture. Two quality control (QC) standards were prepared by adding 100 µL and 30 µL respectively of a mixture containing the analytes of interest (DPA, ABAGE, PA, 7'OH-ABA, neoPA, ABA, and trans-ABA), each at a concentration of 0.2 ng/µL, to 100 µL of the internal standard mix. Finally, samples, blanks, and QCs were reconstituted in an aqueous solution of 40% methanol (v/v), containing 0.5% acetic acid and 0.1 ng/µL of each of the recovery standards (d6-ABA and d2-ABAGE) and subjected to UPLC/ESI-MS/MS analysis and quantification, as described below.

Quantification of PA and ABA metabolites by UPLC/MS/MS-Analysis of ABA and metabolites was carried out by

UPLC/ESI-MS/MS utilizing a Waters ACQUITY UPLC system, equipped with a binary solvent delivery system, column and sample manager coupled to a Waters Micromass Quattro Premier XE quadrupole tandem mass spectrometer via a Z-spray interface as previously described (1,13,14,31,32) .

The analytical UPLC column used was an ACQUITY UPLC® HSS C18 (2.1x100 mm, 1.8 µm) with an ACQUITY HSS C18 VanGuard Pre-column (2.1 x 5 mm, 1.8 µm). The mobile phase A contained 0.025% glacial acetic acid in HPLC-grade water while mobile phase B contained 0.025% glacial acetic acid in HPLC-grade acetonitrile. Sample volumes of 10 µL were injected onto the column at a flow rate of 0.40 mL/min under initial conditions of 2% mobile phase B, which was maintained for 0.2 min, increased to 15% mobile phase B at 0.4 min, then increased to 50% mobile phase B at 5 min and up to 100% by 5.5 min. Mobile phase B was maintained to 100% up to 6.2 min and then decreased to 2% after 6.5 min and held until 8 min for column equilibration before the next injection.

The mass spectrometer was set to collect data in Multiple Reaction Monitoring (MRM) mode controlled by MassLynx v4.1 (Waters Inc). The analytes were ionized by negative-ion electrospray using the following conditions: capillary potential 1.75 kV; desolvation gas flow 1100 L/h; cone gas flow 150L/h; and source and desolvation gas temperatures at 120 ^{o}C and 350 ^{o}C, respectively. The resulting chromatographic traces are quantified off-line by the QuanLynx v4.1 software (Waters Inc). Calibration curves were created for all compounds of interest. Quality control samples (QCs) were run along with the tissue samples.

Enantioseparation of (-)-PA from (+)-PA by UPLC/MS/MS-The enantioseparation of PA was conducted on the same UPLC/MS instrument as described above, using the analytical chiral column Regis (R,R) Whelko 5/100 Kromasil (4.6 x 150 mm, 5 µm, REGIS Technologies, INC). Mobile phase A comprised of 0.1% acetic acid in HPLC-grade water and the mobile phase B comprised of 0.1% acetic acid in HPLC-grade methanol were used. Sample volumes of 15 µL were injected onto the column at a flow rate of 0.40 mL/min under initial conditions of 55% mobile phase B, which was maintained for 1 min, then increased to 90% mobile phase B after 18 min and up to 100% mobile phase B after 19 min. 100% mobile phase B was maintained until 20 min then decreased to 55% by 21 min and held constant until 25 min for column equilibration before the next injection. Under these chromatographic conditions the retention time of synthetic standards of natural (-)-PA and unnatural mirror-image form (+)-PA were 13.0 min and 12.2 min, respectively.

Cortical neuronal cultures-Primary cortical neurons were prepared from embryonic E15-16 CD1 mice and cultured in neurobasal media supplemented with B-27 and N2 (Invitrogen Canada) for 7 - 14 days as previously described (20,24,25). Neurons in these cultures are fully mature and are responsive to glutamate induced excitotoxicity. Briefly, hemispheres were explanted and cleaned free of meninges. Mechanical and enzymatic dissociation in a 0.025% w/v trypsin solution for 25 min followed. A trypsin inhibitor was then added to block the enzyme and 0.05% w/v DNase was added to remove DNA from dead cells. A series of trituration and mild centrifugation steps were included to disperse the neurons prior to resuspension in medium, and to remove undissociated debris prior to plating. Cells were plated onto 24-well plates containing poly-L-lysine coated coverslips at a density of 6 x 10^5 cells per well. Cultures in 100 mm dishes were seeded with 2 x 10^7 cells in 10 ml of culture medium. Cells were incubated at 37 °C.

Neuronal viability assay-After 7 days-in-vitro, cortical neurons were treated with ABA for 15 min prior to the addition of 100 µM NMDA at 37 °C. The plates were then incubated for up to 24 h at 37 °C. Untreated cells were also included as controls. At the end of the treatment period, cells were either fixed for staining or subjected to a neuronal viability assay using Alamar Blue (Invitrogen). Stained cells were examined

under a fluorescent microscope (Carl Zeiss, AX10 vert 200M), and digital images were taken and analyzed using Image J software (http://rsbweb.nih.gov/ij/). The viability of cortical neurons treated with glutamate, and with or without ABAs as mentioned, was assayed using an Alamar Blue assay (Invitrogen). Briefly, a 1:10 dilution of Alamar blue was added to cells for 1 h at 37 °C. The medium was removed and read in a 96-well plate using a plate reader with λEx = 530 nm and λEm = 590 nm. Triplicate readings were obtained per experiment with three independent repeats.

Ratiometric measurement of $[Ca^{2+}]i$ using Fura-2--A ratiometric measurement of $[Ca^{2+}]i$ was performed using Fura-2 AM (25,33). Briefly, mouse cortical neurons at 7 days-in-vitro on glass coverslips were loaded with 5 μM Fura-2-AM (Molecular Probes, Eugene, CA) plus 0.02% pluronic (Molecular Probes, Eugene, USA) for 30 min at 37 °C. After rinsing with PSS Mg^{2+} free buffer containing 2 mM HEPES (pH 7.2), 140 mM NaCl, 5mM KCl, 2.3 mM $CaCl_2$, and 10 mM glucose, stabilized in the same buffer for 5 min, Fura-2 intensities were measured using a Northern Eclipse Digital Ratio Image System (EMPIX, Mississauga, ON) with an Axiovert 200 camera and light source (Zeiss, Thornwood, NY). Fura-2 fluorescence was measured at 510 nm emission with 340/380 nm dual excitation selected by a DG-5 system (Sutter Instrument Company, Novato, CA). $[Ca^{2+}]i$ concentration was represented by the ratio of florescence intensities between the two excitation wavelengths of R340/380 of Fura-2 after a correction for background. The R340/380 for 10 cells in one field of each coverslip was averaged. The basal level of $[Ca^{2+}]i$ was recorded for 20 sec, followed by the application of inhibitors and ABAs. Glutamate (100 μM) was dissolved in PSS buffer and was added to cortical neurons. $[Ca^{2+}]i$ was recorded for 60 - 100 sec. After washing with PSS buffer for 300 sec, PSS buffer containing 45 mM KCl was added to neurons to record changes in $[Ca^{2+}]i$ for 60 sec to show the viability of the neurons. All measurements were repeated for at least 3 times. The data was analyzed using Microsoft Excel and presented as the mean of three experiments.

Whole-cell electrophysiological recordings-Whole-cell patch-clamp recordings were carried out at room temperature (22–25°C) using an Axopatch 700A patch-clamp amplifier (Axon Instruments, Inverurie, Scotland). Data acquisition was achieved using a DigiData 1322A with pClamp 9.0 software. The acquisition rate was 10 kHz and signals were filtered at 5 kHz. Patch electrodes were pulled with a Flaming/Brown micropipette puller (Sutter Instruments, Novato, CA) and fire-polished. The recording electrodes had a resistance of 4–6 MΩ when filled with different internal solutions. For the voltage-clamp recordings, the capacity transients were cancelled using the resistance capacitance circuit within the amplifier. After the formation of whole-cell configuration, access resistances were generally <15 MΩ. Series resistance compensation was set to 70%–90%. The liquid junction potential was approximately 2 mV and was auto-adjusted each time by pipette offset. To record NMDA/AMPA-activated currents, the external solution [(containing (mM): NaCl 150, KCl 5, $CaCl_2$ 0.2, glucose 10 and HEPES 10, pH adjusted to 7.4 with NaOH)] and the pipette solution [containing (mM): KCl 140, $MgCl_2$ 2.5, HEPES 10, EGTA 11, ATP 5, pH adjusted to 7.3 with KOH] were used. For voltage-clamp recordings, the membrane potential was held at −70 mV, unless noted otherwise. Drug solutions were prepared in extracellular solutions and applied to neurons by pressure using the 8-Channel Focal Perfusion System (ALA Scientific Instruments, Farmingdale, NY). Neurons were bathed constantly in extracellular solution between drug applications. Drug solution exchange was accomplished by electronic control.

Patch-clamp data was processed using Clampfit 9.0 (Axon Instruments) and then analyzed in Origin 7.5 (OriginLab, Northampton, MA). The dose-response curve was fitted to the logistic equation: $y=(A1–A2)/[1+ (x/x0)p]+A2$, where y is the response, A1 and A2 are the maximum and minimum

response, respectively, x0 is the concentration corresponding to half-maximal effect, x is the drug concentration, and p is the Hill coefficient.

Indirect immunofluorescence staining and confocal microscopy-The procedures for indirect immunofluorescence immunocytochemistry were exactly as described previously (20,22). Mouse monoclonal antibody to PA was a kind gift from Prof E.W. Weiler (Department of Plant Physiology, Ruhr-University Bochum, Germany) as previously described (12,34). The antibody to PA was diluted with distilled water to 0.2 mg/ml and used at a 1:50 dilution. The primary antibody was incubated with the tissue section in a humidified chamber overnight at 4°C. Sections were then washed 3 times with 10 mM PBS for 10 min and incubated with a rhodamine-conjugated secondary antibody (Invitrogen, Carlsbad, CA, USA) at a concentration of 1:5000 diluted in antibody buffer for 1 h at room temperature. For double immunostaining, after washing with PBS, primary antibodies to CD31, Iba1, MAP2, GFAP, NeuN (see Table 1) were incubated with the section at room temperature for 1 h. Fluorescein-conjugated anti-rabbit or goat secondary antibody against these marker proteins (listed in Table 1) were incubated with the section for 1 h at room temperature.

Sections were then washed 3 times in 10 mM PBS for 10 min, mounted with Dako fluorescent mounting media, spiked with 2 µg/ml Hoechst 33258 (Sigma, Toronto, ON, Canada) to counter stain nuclei. Some sections omitted the primary antibody incubation as a negative control. Confocal imaging was carried out on an Olympus Fluoview FV1000 confocal laser scanning microscope (Olympus, Markham, ON, Canada). Imaging was performed with a 20 X or 40X objective.

Tissue laser-capture microdissection-Laser-capture microdissection was conducted with a Laser Microdissection Leica LMD6 system (Leica microsystems), using 10 infrared and two ultraviolet pulses. Areas of interests were dissected successively from the same brain slide, all cells from the same region being pooled in a single LCM colleting tube. Cells were lysed immediately after dissection and stored at −20°C before UPLC/MS/MS analysis.

Infusion of (-)-PA and (-)-PA antibody into the brain ventricles-Mini-pumps, with an infusion rate of 1.0 µl/hr and a reservoir with up to 3 days delivery capacity (Alzet 1003D) (DURECT Corporation, ALZET Osmotic Pumps, Cupertino, CA) were loaded with (-)-PA (50 mg/ml) or 100% saline (placebo) as described (35). The pumps were submerged in 0.9% sterile saline solution at 37 °C overnight in order to prime them so that (-)-PA was delivered immediately after implantation. Mini-pumps were pre-implanted subcutaneously in the back immediately before the MCAO surgery.

Data analysis-Data was analyzed using Microsoft Excel and Prism 5.0. Statistical significance was determined either by a paired t-test or by one way ANOVA and the significant group was determined using a *post hoc* Tukey's test. $P < 0.05$ was considered statistically significant.

ACKNOWLEDGMENTS: We thank NRC animal facility for the timely supply of animals. We are especially grateful to Prof E. W. Weiler and Mr K. Hagemann (Department of Plant Physiology, Ruhr-University Bochum) for the generous gift of PA antibody. We also thank Amy Aylsworth for meticulously proof-reading of the draft manuscript, and Vera Cekic and Monika Lafond for their technical assistance with hormone profiling sample preparation. Animal antibody work was assisted by Lu Zhang and Yancheng Tang. Patch clamping work was assisted by Lifeng Zheng, Mei Yu and Dr Ying Wang. Financial supports to this project to Dr Shengtao Hou were from the National Natural Science Foundation of China Grant (81571287), Shenzhen Science and Technology Innovation Committee Basic Science Research Grant (JCYJ20140417105742709, JCYJ20160301112230218); State Key Laboratory of Neuroscience Open Competition Grant

(SKLN-201403), SUSTech Peacock Program Start-up Fund to STH (22/Y01226109) and SUSTech Brain Research Centre Fund .

AUTHORS CONTRIBUTIONS: SXJ performed animal brain tissue, blood and CSF collections, preparation these samples for analysis, TTC staining, infarct quantification, hypothermia treatment, and behavioural analysis; JS performed rat and mouse MCAO; XH performed UPLC/MS/MS analysis, LIZ performed data analysis and results interpretation, CLB provided some data analysis and discussion. STH and SA conceived the idea, provided financial support to the project, discussed the data and analysed the results. STH wrote the paper.

COMPETING FINANCIAL INTERESTS: The authors declare no competing financial interests.

References

1. Krochko, J. E., Abrams, G. D., Loewen, M. K., Abrams, S. R., and Cutler, A. J. (1998) (+)-Abscisic acid 8'-hydroxylase is a cytochrome P450 monooxygenase. *Plant Physiol* **118**, 849-860
2. Desikan, R., Cheung, M. K., Bright, J., Henson, D., Hancock, J. T., and Neill, S. J. (2004) ABA, hydrogen peroxide and nitric oxide signalling in stomatal guard cells. *J. Exp. Bot* **55**, 205-212
3. Israelsson, M., Siegel, R. S., Young, J., Hashimoto, M., Iba, K., and Schroeder, J. I. (2006) Guard cell ABA and CO2 signaling network updates and Ca2+ sensor priming hypothesis. *Curr. Opin. Plant Biol* **9**, 654-663
4. White, P. J. (2000) Calcium channels in higher plants. *Biochim. Biophys. Acta* **1465**, 171-189
5. Seiler, C., Harshavardhan, V. T., Rajesh, K., Reddy, P. S., Strickert, M., Rolletschek, H., Scholz, U., Wobus, U., and Sreenivasulu, N. (2011) ABA biosynthesis and degradation contributing to ABA homeostasis during barley seed development under control and terminal drought-stress conditions. *J Exp. Bot* **62**, 2615-2632
6. Hou, S. T., and MacManus, J. P. (2002) Molecular mechanisms of cerebral ischemia-induced neuronal death. *Int. Rev. Cytol* **221**, 93-148
7. Moskowitz, M. A., Lo, E. H., and Iadecola, C. (2010) The science of stroke: mechanisms in search of treatments. *Neuron* **67**, 181-198
8. Papadakis, M., Hadley, G., Xilouri, M., Hoyte, L. C., Nagel, S., McMenamin, M. M., Tsaknakis, G., Watt, S. M., Drakesmith, C. W., Chen, R., Wood, M. J., Zhao, Z., Kessler, B., Vekrellis, K., and Buchan, A. M. (2013) Tsc1 (hamartin) confers neuroprotection against ischemia by inducing autophagy. *Nat Med* **19**, 351-357
9. Lipton, S. A. (2006) Paradigm shift in neuroprotection by NMDA receptor blockade: memantine and beyond. *Nat. Rev. Drug Discov* **5**, 160-170
10. Lipton, S. A. (2007) Pathologically activated therapeutics for neuroprotection. *Nat. Rev. Neurosci* **8**, 803-808
11. Le Page-Degivry, M. T., Bidard, J. N., Rouvier, E., Bulard, C., and Lazdunski, M. (1986) Presence of abscisic acid, a phytohormone, in the mammalian brain. *Proc. Natl. Acad. Sci. U. S. A* **83**, 1155-1158
12. Gergs, U., Hagemann, K., Zeevaart, J. A. D., and Weiler, E. W. (1993) The determination of phaseic acid by monoclonal antibody-based enzyme immunoassay. *Bot. Acta* **106**, 404-410
13. Zaharia, L. I., Galka, M. M., Ambrose, S. J., and Abrams, S. R. (2005) Preparation of deuterated abscisic acid metabolites for use in mass spectrometry and feeding studies. *J Label Cmpd Radiopharm* **48**, 438-445
14. Zaharia, L. I., walker-Simmon, M. M., rodriguez, C. N., and Abrams, S. R. (2005) Chemistry of Abscisic Acid, Abscisic Acid Catabolites and Analogs. *J Plant Growth Regul* **24**, 274-284
15. Balsevich, J. J., Cutler, A. J., Lamb, N., Friesen, L. J., Kurz, E. U., Perras, M. R., and Abrams, S. R. (1994) Response of Cultured Maize Cells to (+)-Abscisic Acid, (-)-Abscisic Acid, and Their Metabolites. *Plant Physiol* **106**, 135-142
16. Abrams, S. R., Nelson, K., and Ambrose, S. J. (2013) Deuterated abscisic acid analogs for mass spectrometry and metabolism studies. *J Label Compd Radiopharm* **46**, 273-283
17. Fisher, M., Feuerstein, G., Howells, D. W., Hurn, P. D., Kent, T. A., Savitz, S. I., Lo, E. H., and Group, S. (2009) Update of the stroke therapy academic industry roundtable preclinical recommendations. *Stroke* **40**, 2244-2250

18. Saver, J. L., Albers, G. W., Dunn, B., Johnston, K. C., Fisher, M., and Consortium, S. V. (2009) Stroke Therapy Academic Industry Roundtable (STAIR) recommendations for extended window acute stroke therapy trials. *Stroke* **40**, 2594-2600
19. Kilkenny, C., Browne, W., Cuthill, I. C., Emerson, M., Altman, D. G., National Centre for the Replacement, R., and Reduction of Amimals in, R. (2011) Animal research: reporting in vivo experiments--the ARRIVE guidelines. *J Cereb Blood Flow Metab* **31**, 991-993
20. Hou, S. T., Jiang, S. X., Desbois, A., Huang, D., Kelly, J., Tessier, L., Karchewski, L., and Kappler, J. (2006) Calpain-cleaved collapsin response mediator protein-3 induces neuronal death after glutamate toxicity and cerebral ischemia. *J. Neurosci* **26**, 2241-2249
21. Hou, S. T., Keklikian, A., Slinn, J., O'Hare, M., Jiang, S. X., and Aylsworth, A. (2008) Sustained up-regulation of semaphorin 3A, Neuropilin1, and doublecortin expression in ischemic mouse brain during long-term recovery. *Biochem. Biophys. Res. Commun* **367**, 109-115
22. Hou, S. T., Jiang, S. X., Aylsworth, A., Ferguson, G., Slinn, J., Hu, H., Leung, T., Kappler, J., and Kaibuchi, K. (2009) CaMKII phosphorylates collapsin response mediator protein 2 and modulates axonal damage during glutamate excitotoxicity. *J Neurochem* **111**, 870-881
23. Hou, S. T., Jiang, S. X., Slinn, J., O'Hare, M., and Karchewski, L. (2010) Neuropilin 2 deficiency does not affect cortical neuronal viability in response to oxygen-glucose-deprivation and transient middle cerebral artery occlusion. *Neurosci. Res* **66**, 396-401
24. Hou, S. T., Jiang, S. X., Aylsworth, A., Cooke, M., and Zhou, L. (2013) Collapsin response mediator protein 3 deacetylates histone H4 to mediate nuclear condensation and neuronal death. *Sci. Rep* **3**, 1350
25. Jiang, S. X., Lertvorachon, J., Hou, S. T., Konishi, Y., Webster, J., Mealing, G., Brunette, E., Tauskela, J., and Preston, E. (2005) Chlortetracycline and demeclocycline inhibit calpains and protect mouse neurons against glutamate toxicity and cerebral ischemia. *J. Biol. Chem* **280**, 33811-33818
26. Jiang, S. X., Kappler, J., Zurakowski, B., Desbois, A., Aylsworth, A., and Hou, S. T. (2007) Calpain cleavage of collapsin response mediator proteins in ischemic mouse brain. *Eur. J. Neurosci* **26**, 801-809
27. MacManus, J. P., Hill, I. E., Huang, Z. G., Rasquinha, I., Xue, D., and Buchan, A. M. (1994) DNA damage consistent with apoptosis in transient focal ischaemic neocortex. *Neuroreport* **5**, 493-496
28. MacManus, J. P., Buchan, A. M., Hill, I. E., Rasquinha, I., and Preston, E. (1993) Global ischemia can cause DNA fragmentation indicative of apoptosis in rat brain. *Neurosci. Lett* **164**, 89-92
29. Tu, Y., Hou, S. T., Huang, Z., Robertson, G. S., and MacManus, J. P. (1998) Increased Mdm2 expression in rat brain after transient middle cerebral artery occlusion. *J. Cereb. Blood Flow Metab* **18**, 658-669
30. Jiang, S. X., Sheldrick, M., Desbois, A., Slinn, J., and Hou, S. T. (2007) Neuropilin-1 is a direct target of the transcription factor E2F1 during cerebral ischemia-induced neuronal death in vivo. *Mol. Cell Biol* **27**, 1696-1705
31. Ross, A. R., Ambrose, S. J., Cutler, A. J., Feurtado, J. A., Kermode, A. R., Nelson, K., Zhou, R., and Abrams, S. R. (2004) Determination of endogenous and supplied deuterated abscisic acid in plant tissues by high-performance liquid chromatography-electrospray ionization tandem mass spectrometry with multiple reaction monitoring. *Anal. Biochem* **329**, 324-333

32. Zaharia, L. I., Gai, Y., Nelson, K. M., Ambrose, S. J., and Abrams, S. R. (2004) Oxidation of 8'-hydroxy abscisic acid in Black Mexican Sweet maize cell suspension cultures. *Phytochemistry* **65**, 3199-3209
33. Jiang, S. X., Benson, C. L., Zaharia, L. I., Abrams, S. R., and Hou, S. T. (2010) Abscisic acid does not evoke calcium influx in murine primary microglia and immortalised murine microglial BV-2 and N9 cells. *Biochem. Biophys. Res. Commun* **401**, 435-439
34. Eberle, J., Arnscheidt, A., Klix, D., and Weiler, E. W. (1986) Monoclonal Antibodies to Plant Growth Regulators: III. Zeatinriboside and Dihydrozeatinriboside. *Plant Physiol* **81**, 516-521
35. DeVos, S. L., and Miller, T. M. (2013) Direct intraventricular delivery of drugs to the rodent central nervous system. *J. Vis. Exp*, e50326

FOOTNOTES

‡ **Current address:** Dr. Suzanne Abrams, Saskatchewan Structural Sciences Centre, Rm 190 Thorvaldson Building, 110 Science Place, University of Saskatchewan, Saskatoon, SK S7N 5C9, Canada

The abbreviations used: ABA, abscisic acid; DPA, dihydrophaseic acid; ABAGE, abscisic acid glucose ester; PA, phaseic acid, 7'OH-ABA, 7'-hydroxy-abscisic acid; *neo*-PA, *neo*-phaseic acid; *cis*-ABA, *cis*-abscisic acid; *trans*-ABA, *trans*-abscisic acid; DW, dry weight; NMDA, N-methyl-D-aspartic acid; CSF, cerebrospinal fluid; LPS, lipopolysaccharides; MCAO, middle cerebral artery occlusion; TTC, 2,3,5-triphenyltetrazolium chloride.

FIGURE LEGENDS

FIGURE 1. Identification and characterization of PA in rodent brains. Chemical structures of (+)-PA and (-)-PA are shown in (A). Near baseline enantioseparation of PA in standard solutions was achieved by a gradient elution mode as described in the Material and Methods section. Brain and blood samples were run on the UPLC/MS/MS using a chiral column and chromatography then compared to that of known standards shown in (B). Spiking experiments of brain and blood samples with known amounts of standards were also performed to confirm that only naturally occurring (-)-PA is present in mouse (B,C) and rat (D) tissues.

FIGURE 2. (-)-PA is endogenously produced in the brain. Mouse brain tissue, blood and mouse food pellets were collected, freeze-dried and subjected to UPLC/MS/MS as described in the Methods section. PA, ABA and its metabolites from mouse brain tissue (A), blood (A) and mouse food pellets (B) were quantitatively determined against dry tissue weight (DW). ** indicates statistical significance ($P < 0.01$ by paired t-test; n = 4 for blood; n = 15 for brain tissues). Both (+)-ABA and (-)-ABA at a dose of 45 mg/kg each were injected into mouse vein. After 2 h and 5 h, brains were collected to determine the level of PA and other ABA metabolites in the brain as shown in panel C. Data represents the mean ± SEM, ** indicates statistical significance ($P < 0.01$ by paired t-test; n = 3).

FIGURE 3. The presence of PA in the choroid plexus and vascular endothelial cells. Immunofluorescent staining with a monoclonal antibody to PA under a confocal microscope showed a clear PA positivity in the choroid plexus in the cerebral ventricles (red colour, arrows in A and B). Double immunofluorescent staining of PA (red colour) with TTR (yellow in merged image of green with red color in B'), DAPI (C; blue colour), CD31 (D; green colour), lectin (G; green colour), PDGFRβ (J; green colour), GFAP (K; green colour), NeuN (L; green colour), and microglia (M; red colour) were performed. PA immunostaining was co-localized with those of CD31 and lectin, indicating that PA is expressed by endothelial cells. PA did not show co-localization with pericytes which surrounds the microvessels, nor with astrocytes, microglia and neurons. Scale bars = 50 μm.

FIGURE 4. Cerebral ischemia elevates the level of (-)-PA in the CSF and brain. (A): schematic diagram of MCAO model. The middle cerebral artery was occluded for 1 h and followed by up to 24 d reperfusion. Blood and brain tissues were collected at 2 h, 6 h, 24 h, 6 d and 24 d after reperfusion. CSF was collected after 24 h reperfusion. Samples were subjected to UPLC/MS/MS analysis. (B): Panel shows the elevated (-)-PA level in both the ipsilateral and contralateral side of the ischemic brain. Rat brains were collected after 24 h reperfusion and fold of induction of (-)-PA was determined and presented in (C). CSF and blood were taken after 24 h reperfusion from MCAO rats and the concentration changes were shown in (D). Data represents the mean ± SD, **

indicates $P < 0.05$, *** indicates $P < 0.01$ (one way ANOVA with Tukey's *post hoc* analysis; n = 5).

FIGURE 5. MCAO elevated (-)-PA level in the non-ischemic tissue. An example of coronal section of the ischemic brain is shown in (A). Numbers in the square boxes on (A) indicates areas of interests. PA immunostaining omitting the primary antibody was performed to show tissue specificity (B). The expression of PA in sham-operated mouse brain (C) and ischemic brain (D-I) were examined under a fluorescent microscope. Lectin was labelled as green fluorescence in D, G. Co-localization of lectin with PA is shown in panel I. Laser capture microdissection was used to obtain tissues from areas of interests as indicated in (A). These samples were subjected to UPLC/MS/MS analysis to detect (-)-PA levels. Data represents mean ± SEM, ** indicates $P < 0.05$ compared to area 2 of tissues from the infarct core (one way ANOVA with Tukey's *post hoc* analysis, n = 5).

FIGURE 6. Reversible inhibition of NMDA receptors by (-)-PA. Ratiometric calcium imaging (A): Cultured cortical neurons on glass cover slips were loaded with Fura-2AM for 30 min followed by washing with PSS, or HBSS buffer. (-)-PA at the indicated concentrations was added to neurons. Fura-2 fluorescence from more than 10 selected neurons was measured for up to 30 min. After wash with PSS, or HBSS buffer, NMDA with or without (-)-PA at the indicated dosage was loaded onto neurons. Addition of KCl showed a large [Ca2+]i, confirming that these neurons were functional cells. Changes in calcium were measured by converting the 340/380 ratio of Fura-2 florescence (after correction for background) as described. Data obtained from at least three independent experiments (n = 20 cells) were averaged and plotted (B). Representative NMDA currents activated by 50 μM NMDA plus 1 mM glycine and their inhibition by 100 and 1000 μM (-)-PA (C and D). (-)-PA was first applied for 30 s, and then simultaneously applied with NMDA. Membrane potential was clamped at 270 mV. Panel E shows (-)-PA concentration-response relationship for inhibition of NMDA currents activated by 50 μM NMDA plus 1 μM glycine. Concentration-response curve was fitted by the logistic equation, with the IC 50 of 35.4 ± 1.5 μM and a slope factor of 0.96 ± 0.3 (n = 10). Data in E represents the average of 10 neurons. Data represents the mean ± SEM, ** indicates $P < 0.05$ compared to NMDA group in (B) using one way ANOVA with Tukey's *post hoc* analysis, n = 20.

FIGURE 7. (-)-PA protects cultured cortical neurons against glutamate toxicity and reduces ischemic brain injury. Neuronal viability was assessed using Alamar blue assay. NMDA at 100 μM reduced cellular viability to 40% compared to the untreated control (A). (-)-PA alone has no toxicity to neurons (A). Adding (-)-PA to NMDA treated neurons significantly protected cells from death (B). DAPI staining of cellular nuclei is shown in C. Data represents the mean ± SEM, ** indicates $P < 0.05$, (one way ANOVA with Tukey's *post hoc* analysis; n = 5). (D – F): (-)-PA protects mouse brain from MCAO-induced damage. Mice were subjected to 1 h MCAO and 24 d reperfusion as described in the Methods section. Osmotic pump was pre-implanted before MCAO surgery to deliver (-)-PA into the ischemic side of the brain ventricle as described in the Methods section. (-)-PA was also delivered to non-MCAO mice serving as a control. (D): Mice survival rate was plotted. (-)-PA itself, or administered into MCAO mice, did not alter significantly the survival rate, as this MCAO model has very low death rate to begin with. Brain slices were stained with TTC, soluble TTC was extracted and measured using a spectrophotometer (E). Quantification of TTC staining showed a significant reduction in brain infarction compared with the vehicle-treated mice (E; *$P < 0.05$; paired t-test; n = 11). Neurological deficit scores were also measured at 0.5 h, 6 d and 24 d after MCAO and reperfusion (F). Data represents the mean ± SD and * indicates $P < 0.05$ by paired t-test, n = 11 for 0.5 d and 6 d MCAO groups and the PA-no-MCAO group. n = 10 for the 24 d group).

FIGURE 8. Reduction of (-)-PA level exacerbates brain injury in MCAO mice. Mice were subjected to 1 h MCAO and 24 h reperfusion as described in the Methods section. Osmotic pump was pre-implanted before MCAO surgery to deliver PA monoclonal antibody into the ischemic side of the brain ventricle as described in the Methods section. TTC staining of brain slices are shown in (A). The infarct areas are highlighted with dotted lines (A). The infarct volume at 24 h reperfusion was quantified and shown in (B). Infusion of PA monoclonal antibody significantly increased infarct volume compared with vehicle (saline)-infused ischemic brain. The neurological deficit scores (C) and forepaw pulling strength (D) were also measured and compared amongst the three groups (▲: PA without MCAO; ○:PA Ab with MCAO, and ■: no PA Ab with MCAO). (E): A sample of ischemic brain coronal section highlighting areas of interests. Fluorescent double immunohistochemical staining of ischemic mouse brain infused with PA antibody showed reduced PA immunofluorescence (red colour) both in the ischemic core (F) and the surrounding penumbra (G). Blood vessels were stained with lectin (green colour). For comparison with a control group lacking of PA antibody treatment, please see Fig 5 D, E, F. To confirm this, brain tissues were laser microdissected out from areas 1, 2 and the contralateral side (labelled as right) for UPLC/MS/MS quantification of (-)-PA levels (H). (-)-PA level was significantly reduced in the ischemic side of the brain surrounding the core. Data represents the mean ± SD and ** indicates $P < 0.01$ by paired t-test, n = 5). n.s. = non-significant with $P = 0.2$, one way ANOVA with Tukey's *post hoc* analysis.

FIGURE 9. Known metabolic pathways of (+)-ABA in plants. The principal oxidative pathway of natural (+)-ABA (1), mediated by cytochrome P-450 monooxygenases, occurs through hydroxylation of the 8'-methyl group resulting in 8'-hydroxyABA (2), which rearranges to PA (3). Further enzymatic reduction of PA leads to DPA (4). Other metabolic steps include hydroxylation of the 7' and 9'-methyl groups of the ABA ring as well as the conjugation of glucose esters (ABAGE, 5). In plants, Trans-ABA (6) is a product of isomerisation of natural ABA under UV light. The unnatural mirror-image form of PA (7) may also occur as a result from the feeding of unnatural (-)-ABA.

Figure 1

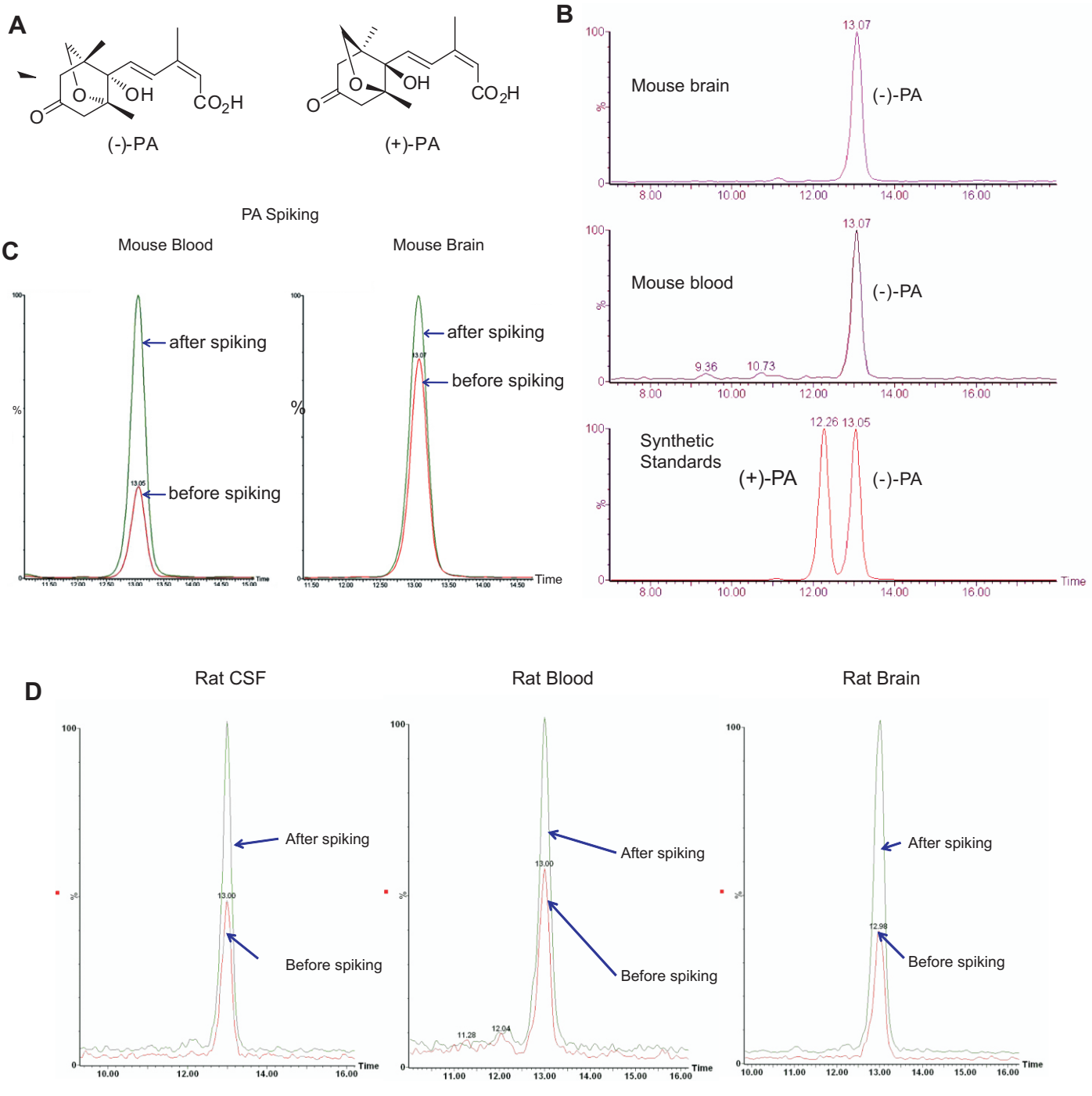

Figure 2

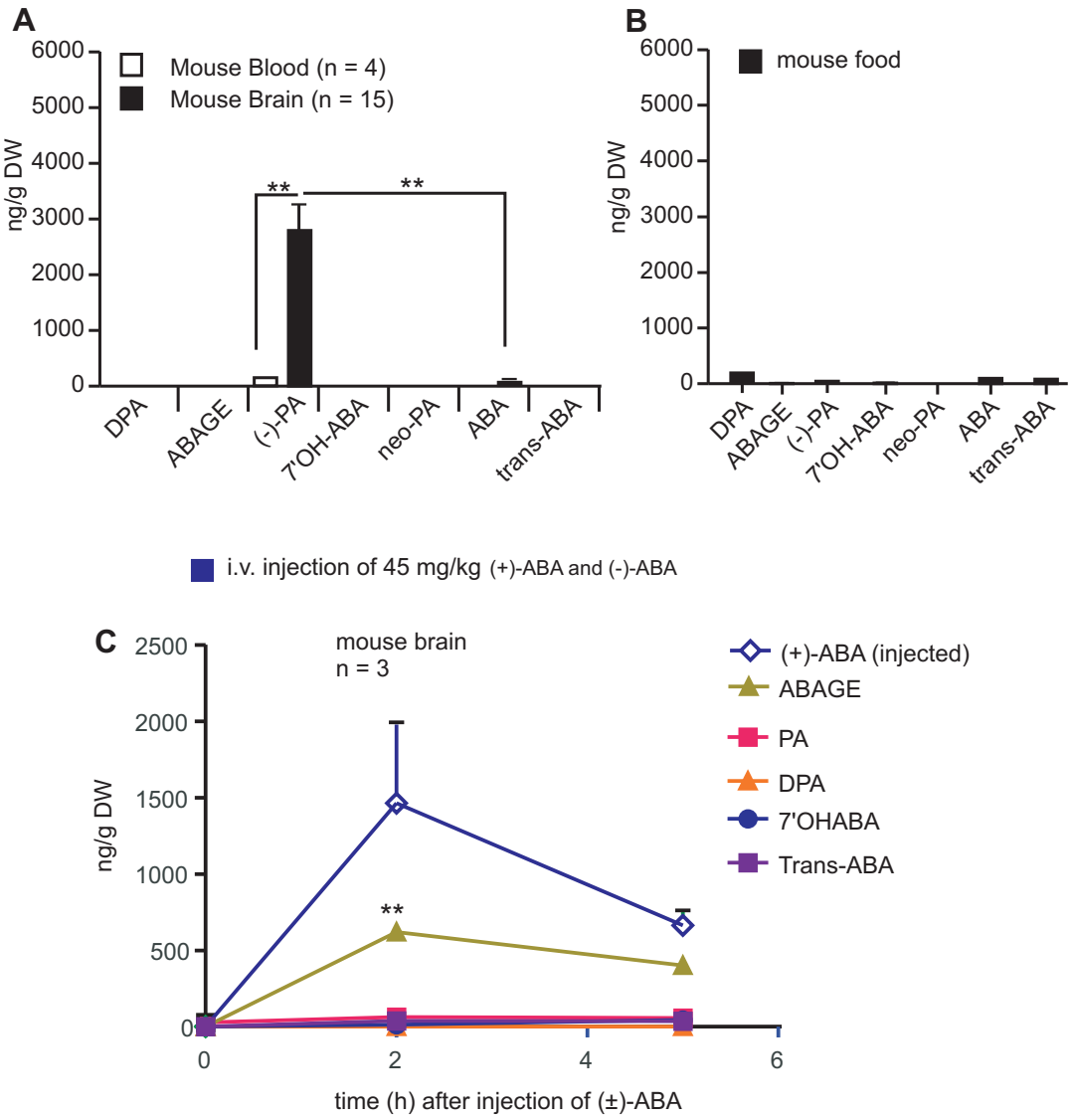

Figure 3

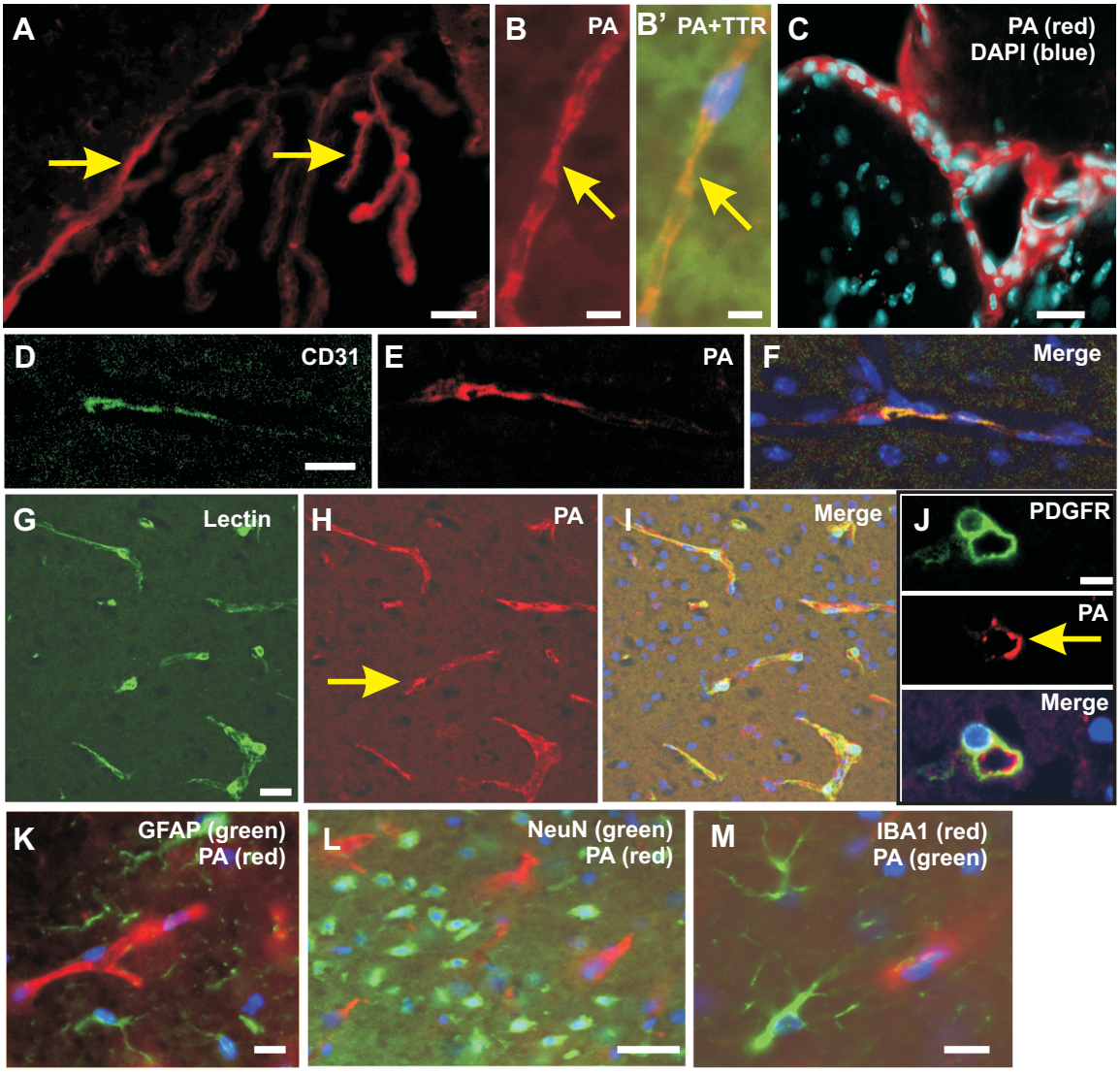

Figure 4

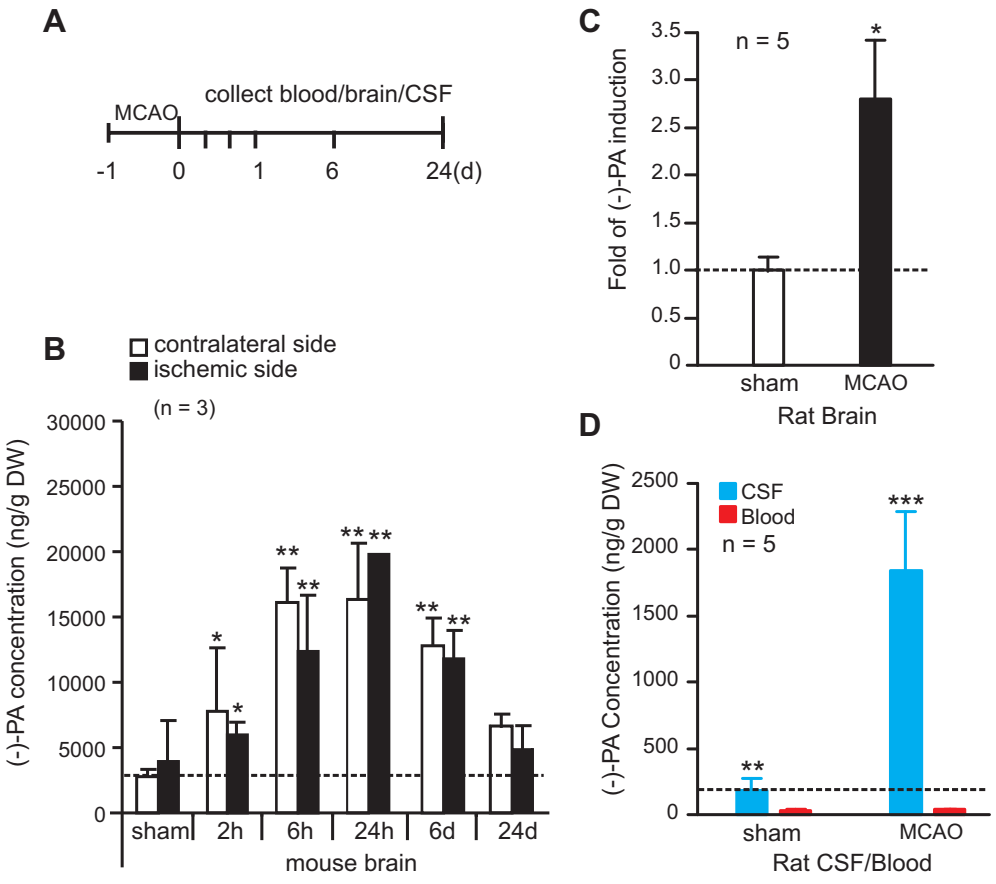

Figure 5

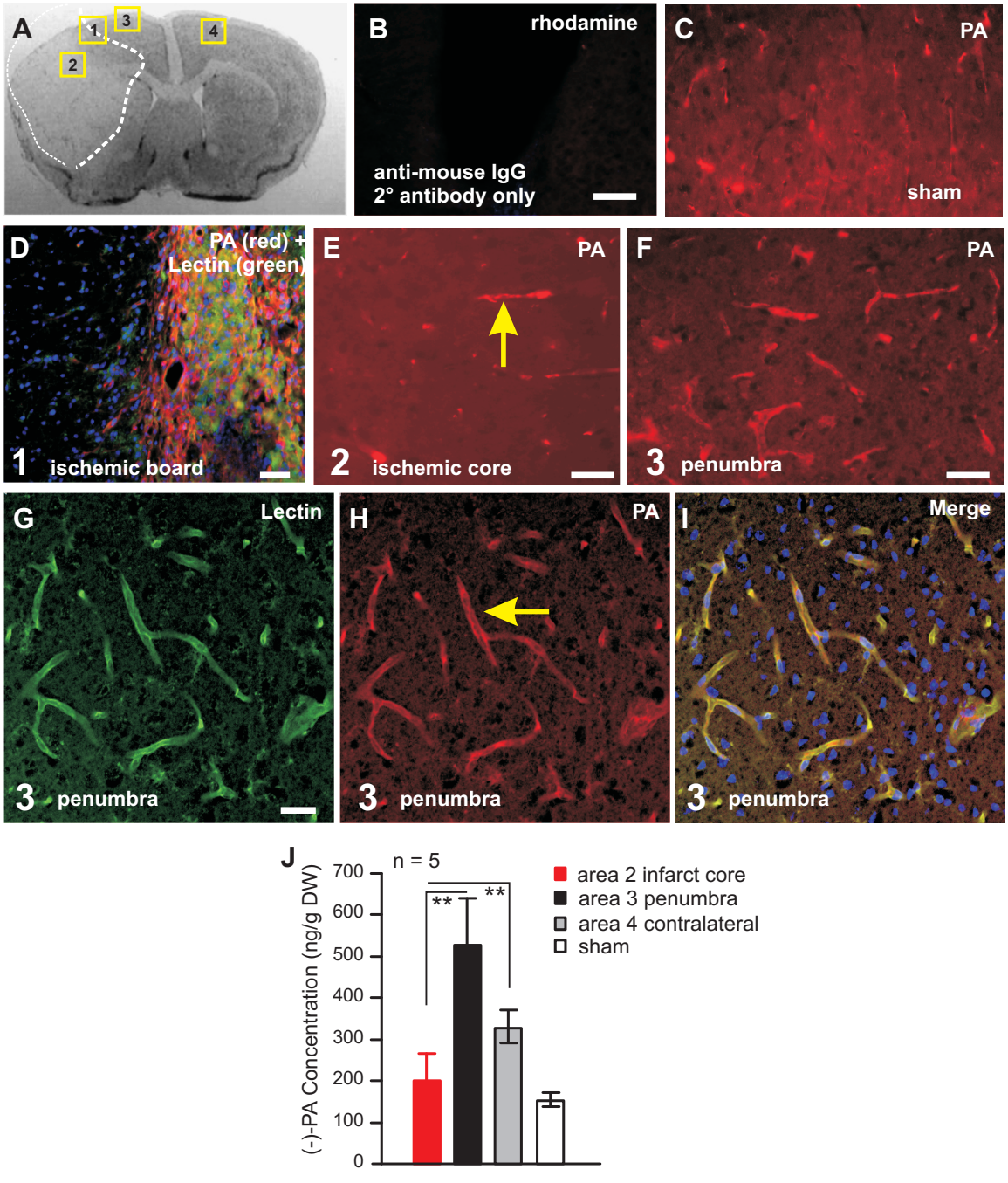

Figure 6

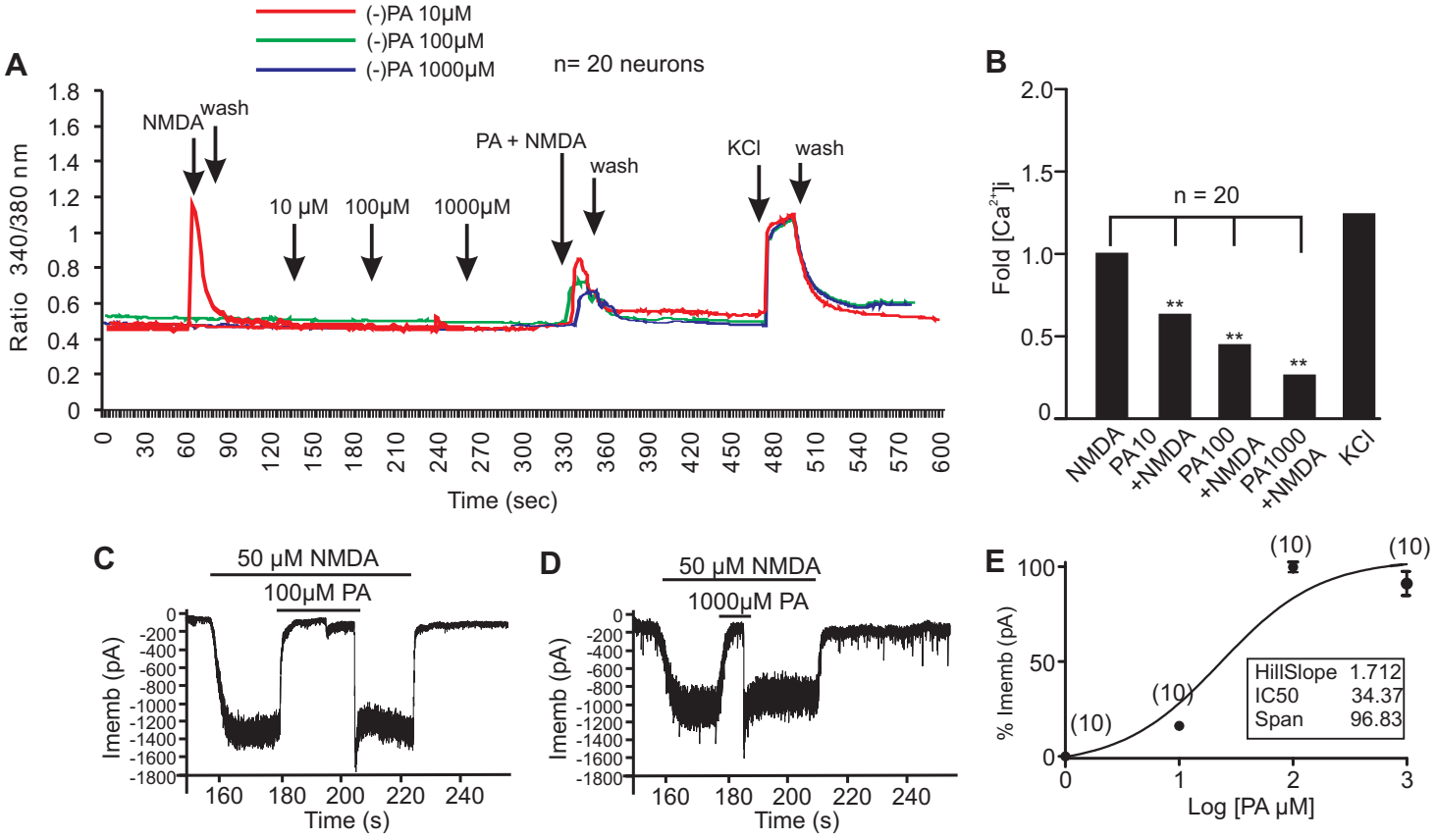

Figure 7

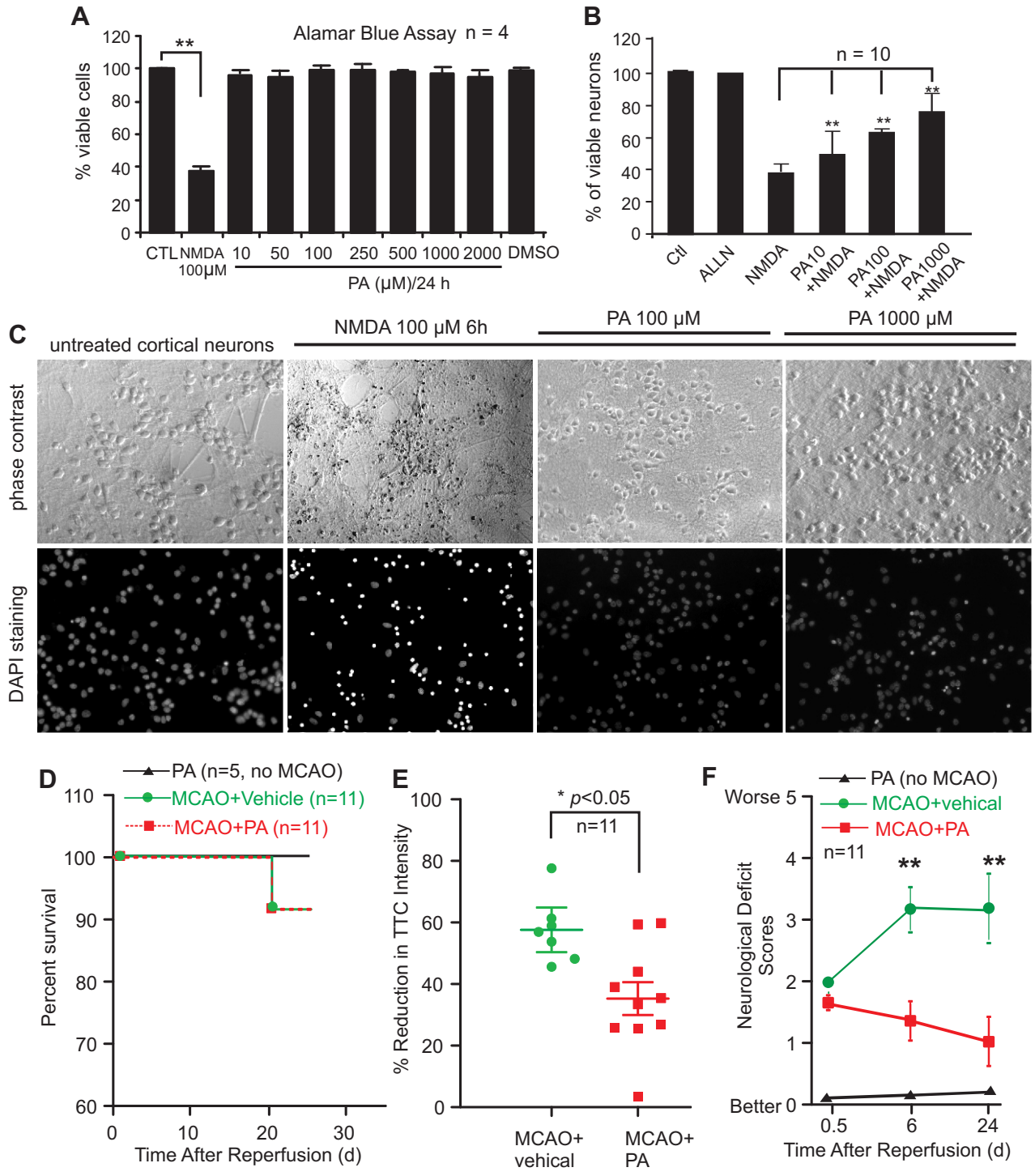

Figure 8

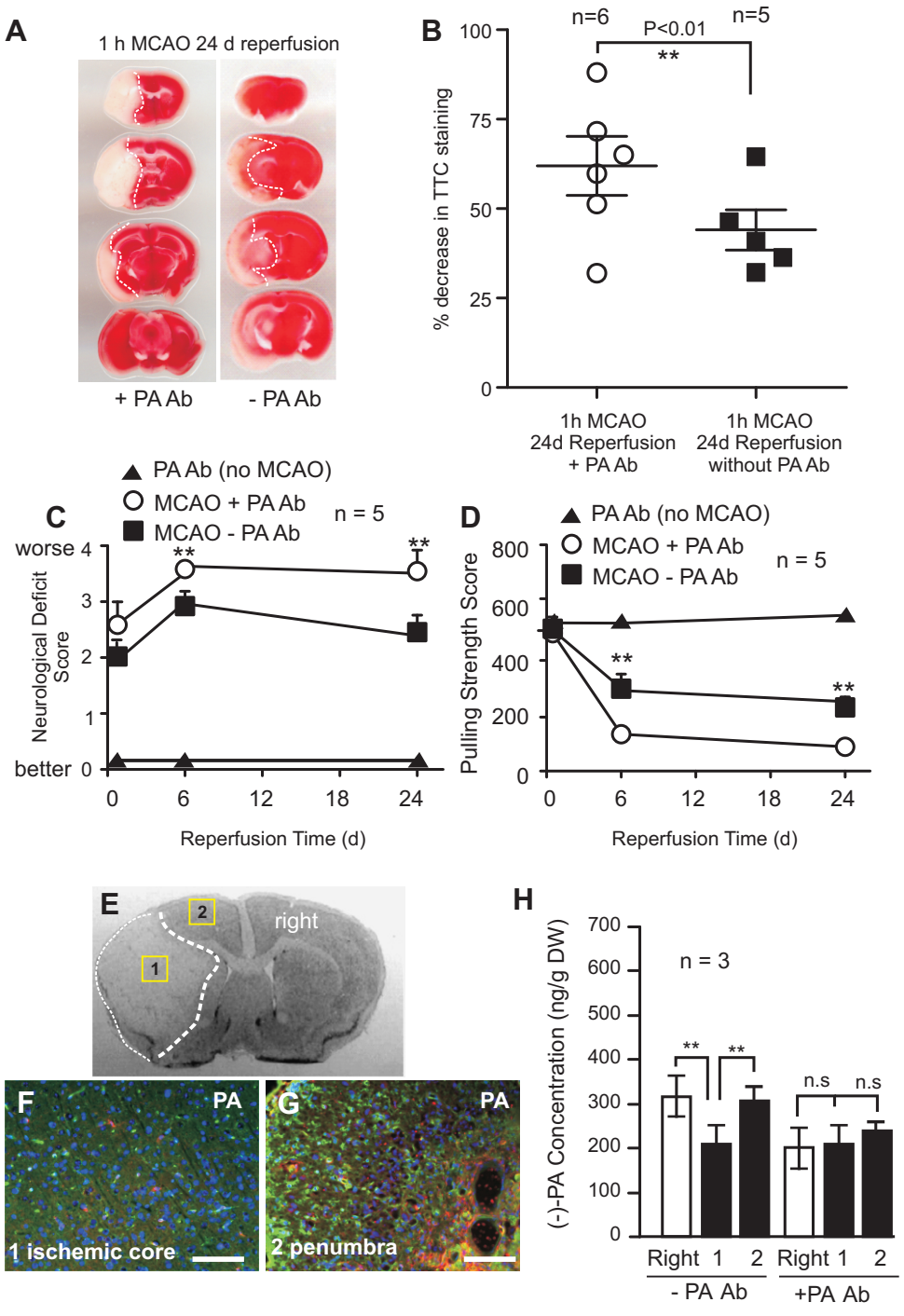

Figure 9

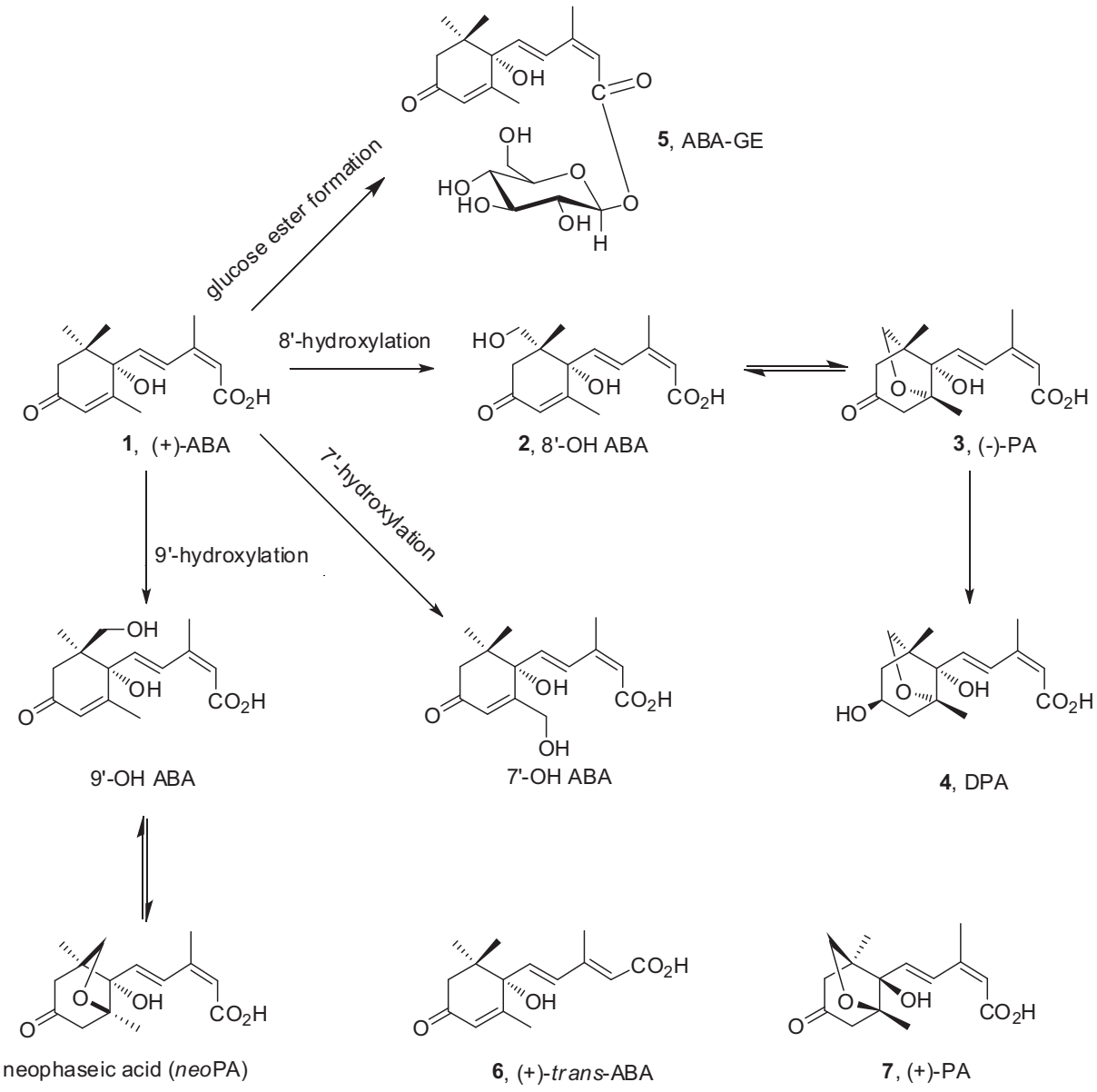

Phaseic Acid: An Endogenous and Reversible Inhibitor of Glutamate Receptors in Mouse Brain

Sheng T. Hou, Susan X. Jiang, L. Irina Zaharia, Xiumei Han, Chantel L. Benson, Jacqueline Slinn and Suzanne R. Abrams

J. Biol. Chem. published online November 18, 2016
